ELSEVIER

Contents lists available at ScienceDirect

# Journal of Materials Research and Technology

journal homepage: www.elsevier.com/locate/jmrt





# Generative hyphal stiffness and cell wall thickening in fungi

James A.L. Gallagher<sup>a</sup>, Jessica N. Redmond<sup>a</sup>, Meisam Asgari<sup>b</sup>, Alexander J. Bradshaw<sup>c</sup>, Bryn T.M. Dentinger<sup>d</sup>, Steven E. Naleway<sup>a,\*</sup>

- <sup>a</sup> Department of Mechanical Engineering, University of Utah, Salt Lake City, 84112, UT, USA
- <sup>b</sup> Department of Medical Engineering, University of South Florida, Tampa, 33620, FL, USA
- <sup>c</sup> Biology Department, Clark University, Worcester, 01610, MA, USA
- d Natural History Museum of Utah & School of Biological Sciences, University of Utah, Salt Lake City, 84112, UT, USA

#### ARTICLE INFO

Handling Editor: P.Y. Chen

Keywords: Biomechanics Fungi Generative hyphae Cellular structures AFM

#### ABSTRACT

Filamentous fungi produce multinucleate, interconnected tubular structures called hyphae which are the building blocks of all fungal structures, including mushrooms and mycelium. This makes hyphae foundational to understanding all fungal mechanics. While there have been studies of the dimensions and mechanical properties of hyphae, research comparing these microstructures has been minimal. This study compares generative hyphae from different hyphal systems to determine what factors may affect their mechanical properties. Three related Polyporales species were studied for their unique hyphal systems: *Sparassis spathulata* (monomitic), *Grifola frondosa* (dimitic), and *Ganoderma sichuanense* (trimitic). Fourier Transform Infrared Spectroscopy showed that chemical compositions were consistent between species. Scanning Electron Microscopy showed a significant decrease in diameters, increased cell wall thickness, and increased material volume percentage from monomitic to dimitic to trimitic species. Overall, cell wall material usage per hyphae remained balanced between species. Transmission Electron Microscopy imaging further illustrated this with increasing cell wall chitin layer growth from monomitic to dimitic to trimitic species. Data showed fungi that grew smaller and thicker hyphae were stiffer than larger and thinner hyphae. Hyphal mechanical properties found in this study could inform applications in high-strength biocomposites and sustainable bioinspired designs.

#### 1. Introduction

Mycelial products are a fast-growing commodity that have a low energy cost to produce and generate minimal waste [1]. For example, mycelium-based bricks are becoming a sustainable alternative in the construction industry for their good thermal insulation and surprising durability [2]. The cause of this durability has become a keen interest in recent years [3,4]. Extensive research has been aimed at elucidating the macroscopic properties of fruiting bodies (i.e. mushrooms) [5,6], yet the mechanical properties of the microscopic structures still need to be unearthed. The most basic unit of fungi is the hypha [7]. It is a tubular, multinucleate structure enclosed by a chitinous cell wall, typically with interconnected cytoplasm in filamentous fungi [4]. These hyphae can form large branching networks called mycelium [8]. More than just the mycelium, hyphae compose almost the entirety of all fungal structures [9]. If one were to look closely at a mushroom, it would appear as millions of interlocking hyphae [9]. The variation of these

microstructures has been shown to affect the overall macrostructure [10, 11]. Thus, examining these hyphae is crucial to understanding the mechanical properties of filamentous fungi at all levels.

One key aspect to understanding hyphae is by looking at the structure of their cell wall [12]. The cell walls of hyphae are complex composite structures that are important for protecting against environmental stresses [4]. It can be functionally and structurally divided into mobile and rigid phases [3]. The mobile phase is often found in the outer portion of the cell wall and consists of a mix of polysaccharides such as mannans, galactomannans, and various glycoproteins, which are used for interacting with the environment [3,13]. The rigid phase of the cell wall is composed of a more heavily cross-linked network of  $\beta$ -(1,3) and  $\beta$ -(1,6) glucans, chitosan, and chitin, which is responsible for the rigidity and strength of the cell wall as well as the cell shape [3,13]. The rigid phase is often found in the inner portion of the cell wall [3,4]. The exact compositions of the cell wall aren't easily quantified, but what is accepted is that the cell wall is a

E-mail address: steven.naleway@mech.utah.edu (S.E. Naleway).

<sup>\*</sup> Corresponding author.

**Table 1** The fungal species used in this study with their common name, and hyphal system with the hyphae they can produce. G = Generative, S = Skeletal, and B = Binding.

| Species Name            | Common Name                     | Hyphal<br>System | G | S | В |  |
|-------------------------|---------------------------------|------------------|---|---|---|--|
| Sparassis spathulata    | Eastern cauliflower<br>mushroom | Monomitic        | Х |   |   |  |
| Grifola frondosa        | Maitake mushroom                | Dimitic          | X | X |   |  |
| Ganoderma<br>sichanense | Reshi mushroom                  | Trimitic         | X | X | X |  |

dynamic structure that can undergo remodeling to introduce new properties to the hyphae [14,15]. Furthermore, fungi have evolved to have a great deal of variability in the dimensions of their hyphae and cell walls between species and sometimes within species [16]. This has led to fungi having a wide range of properties that have allowed them to adapt and survive in many different environments found on Earth [17,18]. There have been studies of the mechanical properties of hyphae, but there has been very little comparative research of these microstructures [19,20]. Comparative analysis of hyphae, their dimensions, material composition, and mechanical properties can help explain differences in the mechanical properties on the micro and potentially the macroscopic scale.

This study looks at Agaricomycetes; a class within the kingdom of Fungi known for producing the fruiting bodies commonly recognized as mushrooms. Within this class, the order Polyporales further contains many Polypores, which have some of the hardest fruiting bodies found in nature, making them of keen interest for the study of their structural properties [14,15,21]. Despite the relatively close genetic relation, Polyporales fungi also produce various hyphae that serve as excellent examples of differing hyphal systems. The most common hyphal type is the generative [22]. They are totipotent which means each cell can develop into any other cell type and are responsible for forming other structures such as the basidia, responsible for spore production and, in some species, other specialized hyphae [23]. There are several ways to identify generative hyphae. They are frequently branched, are septate, meaning they have septa (cell walls with pores separating linked cells) [25,26], and in most cases will form clamp connections. Clamp connections are hook-like structures involved in maintaining two separate nuclei within each hyphal cell and are often visible at the septa if the fungal culture has mated. They are not found on most other cells [27,

In addition to generative hyphae, two other hyphal types have been identified: skeletal and binding hyphae [29]. Skeletal hyphae have been observed to be smaller, longer hyphae that are rarely branched. They often have thick cell walls. Binding hyphae are small, frequently branched, and grow to be interwoven into a coral-like structure. They link together the structure of many Polypore fruiting bodies [28]. Both skeletal and binding hyphae are aseptate [25]. As detailed in Table 1, Fungi with only generative hyphae in their mycelium and fruiting bodies are considered monomitic [29,30]. Fungi with generative hyphae and one additional type of hyphae are considered dimitic. Fungi that produce all three hyphal types are considered trimitic [30]. While skeletal and binding hyphae are interesting, because generative hyphae are present in all three hyphal systems, they are the most important hyphae to examine to understand fungal mechanics. Other variants of hyphae could affect the mechanical properties found in basidiomycetes [31]. Very little literature exists examining the properties of these hyphae and how they differ between species. This has led to studies showing properties of certain fungi as a whole but don't denote the individual contributions of the different types of hyphae to the overall structure [32]. Other literature uses the term generative hyphae, though usually only as a visual classification of observed features, and little work has been done on discerning the material and structural properties of these hyphae [33].

This study characterizes the generative hyphae from mycelial tissue of three related Polyporales species that were chosen to represent monomitic, dimitic, and trimitic hyphal systems. By using Scanning Electron Microscopy (SEM) and Transmission Electron Microscopy (TEM), differences in hyphal size, cell wall thickness, and material usage could be determined between species. These dimensions are insightful in explaining the changes in elastic moduli (Stiffness) found between species. Further study of Fourier Transform Infrared Spectroscopy (FTIR) can compare adsorption spectra between species and determine if the mechanical properties of these hyphae are affected by chemical composition differences. An increased understanding of hyphal structures and their mechanical properties on the microscale can help in understanding the macroscale's mechanical properties and inform applications such as fungal composites and other bioinspired designs.

#### 2. Materials and methods

## 2.1. Species selection, species verification, and sample culturing

Three species were selected for having monomitic, dimitic, and trimitic hyphal systems within the order of Polyporales. Sparassis spathulata was selected as a representative monomitic species for only having generative hyphae in its fruiting body [34]. Sparassis spathulata culture was purchased from The Mycelium Emporium [35]. Grifola frondosa was selected as a representative dimitic species for having both generative and skeletal hyphae in its fruiting body [36]. Ganoderma sichuanense was selected as a representative trimitic species for having generative, skeletal, and binding hyphae in its fruiting body [25]. Grifola frondosa and Ganoderma sichanense cultures were obtained from the Oregon State University College of Forestry. All cultures are in long-term storage and available upon request. Due to the ease at which fungal species are misidentified and per the proposal of Schoch et al. [37], all species underwent a DNA verification to independently confirm the species identity. The internal transcribed space (ITS), the universal DNA barcode for fungi, was used to identify fungal species of isolates through PCR amplification. For amplification of the ITS, the primer combo ITS-8F (5'-AGTCGTAACAAGGTTTCCGTAGGTG-3') was used along with ITS-6R (5'-TTCCCGCTTCACTCGCAGT-3'), which have higher specificity for Agaricomycetes [38,39]. Amplified sequences were then sequenced using Sanger sequencing through the DNA sequencing core at the University of Utah. Using the BLAST algorithm, sequences were compared to the NCBI nucleotide database, GenBank [40,41].

For all experiments conducted in this study, the mycelium was grown with 9 cm petri dishes filled with potato dextrose agar (PDA). PDA plates were prepared in accordance with previous literature [42,43]. Samples were grown at 21 °C for thirty days [44]. Different growing conditions have been shown to influence fungal growth dynamics [45]. This study tested fungi under one growth environment to keep all other variables constant and isolate the effects of species-specific traits on growth behavior [46].

#### 2.2. Scanning Electron Microscopy

Fifteen samples were collected from fifteen petri dishes, with five samples from each of the three species. Each sample consisted of 2 mm  $\times$  2 mm squares of mycelium on agar, cut from the outer edges of the petri dishes with mycelium of the same age using a scalpel. The samples were fixed, dehydrated, and critical point-dried using standard preparation techniques [47]. Samples were fixed using 2.5 % glutaraldehyde, 1 % paraformaldehyde, and 0.1 M sodium cacodylate buffer (pH 7.2) for 24 h at 21 °C. A secondary fixation was applied using 1 % osmium tetroxide, buffered with 0.1 M sodium cacodylate buffer. For measurements of cell wall thickness, the samples were halved along their transverse axis with a razor after the secondary fixation. Critical point drying was conducted with an Autosamdri-815B, Series B (Tousimis, Rockville, USA) at 31 °C and 1072 psi, the critical point of carbon

dioxide, for 4 min. This fixation process aimed to preserve the fungal cell's natural shape and avoid dehydration and collapse of the structure when under vacuum for SEM. After fixation, samples were mounted on specimen stubs with colloidal graphite and coated with 15 nm of gold/palladium using a LEICA CE600 high vacuum sputter coater (Leica, Wetzlar, Germany).

Samples were imaged using a Zeiss GEMINI Scanning Electron Microscope (Zeiss, Orberkochen, Germany) with an electron high tension (EHT) of 15 kV in a high vacuum. Top-down images of the surface plane were taken as a 2D representation of the mycelium and cross-sectional images were taken by cutting the 2 mm  $\times$  2 mm sample squares in half along their transverse plane and mounting them at  $90^{\circ}$  to expose the hyphal cell wall thickness. Images collected in the SEM were measured using ImageJ. Five samples of each species were used for imaging. One-hundred measurements of both diameter and cell wall thicknesses were taken from the cross-sections of generative hyphae. Features that might cause major changes in diameter, such as branching, clamp connections, and noticeable septa, were avoided. Measurements were taken from subapical hyphae. The theoretical material volume of cell wall relative to overall volume was calculated using the cross-sectional area of a pipe equation using the mean diameters and cell wall thicknesses provided above:

$$A = \frac{\pi D^2}{4} - \frac{\pi (D - 2T)^2}{4} \tag{1}$$

where the hyphal diameter is D, and the cell wall thickness of the hyphae is T. The cross-sectional area of the hyphae composing the cell wall material is A.

## 2.3. Transmission Electron Microscopy

An additional three samples were taken from each species and prepared for TEM using a similar procedure to past literature [48,49]. Like sample preparation for SEM, samples were fixed using 2.5 % glutaraldehyde, 1 % paraformaldehyde, and 0.1 M sodium cacodylate buffer (pH 7.2) for 24 h at 21 °C. A secondary fixation was applied using 1 % osmium tetroxide, buffered with 0.1 M sodium cacodylate buffer. Water in the cells were replaced with successive changes of ethanol like the SEM process until ethanol reached 100 %. Instead of critical point drying, ethanol was exchanged with 100 % acetone for three changes for 30 min each. Acetone was exchanged with successive changes of a one-to-one EmbedA12 epoxy resin to acetone for 1 h and then a three-to-one 24 h change. Samples were then given three additional changes of 100 % EmbedA12 with cycles of sitting in EmbedA12 in a closed capped vial on a rocker for 1 h followed by 1 h, cap off under vacuum. Samples were then placed in a final change of EmbedA12 in a flat block mold and placed in a 60 °C oven to harden over 24 h.

Samples were then hand trimmed with razor blades under a dissecting scope for preparation for thin sectioning. Thin sectioning was performed with a Leica Ultracut UCT (Leica, Wetzlar, Germany) with a diamond knife. Sections were collected on 3 mm, two hundred mesh copper grids contrasted with uranyl acetate and Reynold's lead citrate. Images were collected using a JEM-1400+ Transmission electron microscope (JEOL, Akishima, Tokyo, Japan) at 120 kV. Digital images were saved using a Gatan Orius Camera (Gatan, Pleasanton, USA). Images collected in the TEM were measured using ImageJ. Fifteen images of hyphal cross sections of each species were used to measure both the outer mobile portions of the cell wall and the inner rigid portions.

## 2.4. Mechanical testing

A JPK Nanowizard PURE atomic force microscope (Bruker Nano, Berlin, Germany) mounted on an inverted epifluorescence Zeiss Axiovert 200 M microscope (Carl Zeiss Microscopy, Göttingen, Germany) was used for imaging and mechanical characterization of cultured

samples. The samples were imaged using tapping mode and mechanically tested using Quantitative Imaging (QI) Advanced mode in accordance with developed protocols for indentation [50]. All the tests were performed in the dehydrated state. The maximum lateral scan focused on regions measuring 100  $\mu m$  by 100  $\mu m$ , with a scanning rate set to 1 Hz. Reduced scan areas were then selected to obtain detailed structural information of the tissue. For imaging and tissue-indentation measurements, Biosphere Au Reflex Non-Contact High Resonance (NCHR) cantilevers (Nanotools USA LLC, Henderson, NV) with a nominal spring constant of 40 N/m and integrated spherical tip of radius 100 nm ( $\pm 10$ %), a length of 125 μm, and a nominal resonance frequency of 330 kHz in air were employed [51]. The indentation rate was set to  $2 \mu m/s$ . The indentation depth was maintained below 10 nm by minimizing forces to ensure purely elastic, small deformations, with depth-to-sample thickness and depth-to-tip radius ratios kept minimal. Before each test, the deflection sensitivity of the cantilever was calibrated by engaging it on a clean glass slide [52]. The exact spring constant of the cantilever was calibrated using thermal noise fluctuations in air. This was done by fitting the first free resonance peak of the cantilever to that of a simple harmonic oscillator [53] using the JPK software [50]. The AFM force-displacement curves indicated negligible adhesion effect. The elastic modulus was obtained from the Hertzian contact model [54], where the contact radius a is related to the indenting force F through

$$a = \left(\frac{3RF(1 - \nu^2)}{4E}\right)^{1/3} \tag{2}$$

with R being the radius of the spherical tip, and  $\nu$  and E being the Poisson's ratio and elastic modulus of the sample, respectively [54]. The indentation depth  $\delta$  is expressed in terms of the contact radius as

$$\delta = \frac{a^2}{R} = \left(\frac{9F^2(1 - \nu^2)^2}{16RE^2}\right)^{1/3} \tag{3}$$

JPK data processing software was used to analyze the indentation data.

## 2.5. Fourier Transform Infrared Spectroscopy

FTIR analysis was performed to measure the absorbance of chemical bonds by wavenumber for hyphae from all three species using a Nicolet iS50 FTIR Spectrometer (Thermo Fisher Scientific, Waltham, USA) [55, 56]. The hyphae of each species were collected directly from one of their petri dishes with forceps and tested in a hydrated state. This test aimed to determine whether the generative hyphae of each species had a unique chemical composition to one another that could be attributed to changes in mechanical properties between species.

## 2.6. Statistical analysis

Statistical significance was determined by one-way variance analysis (ANOVA) followed by post-hoc analysis using Tukey's Honestly Significant Difference test in R Studio. Pairwise comparisons were conducted for each species sample, with statistical significance determined at a confidence level of  $\alpha=0.01$  These tests were performed on hyphal diameter, thickness, cell wall material volume per length of hyphae, percentage of hyphal volume composed of cell wall, and elastic modulus measurements.

#### 3. Results and discussion

#### 3.1. Species verification

DNA extraction and barcoding successfully verified the three species used in this study. The sequence of the *Sparassis spathulata* culture was 100 % identical to the sequence of a *Sparassis spathulata* in GenBank

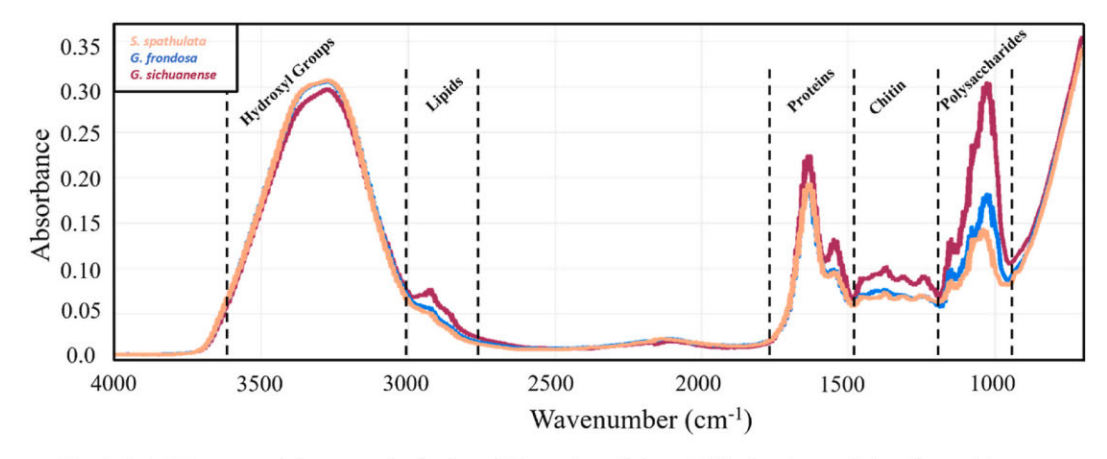


Fig. 1. An FTIR spectra of the generative hyphae of Sparassis spathulata, Grifola frondosa, and Ganoderma sichanense.

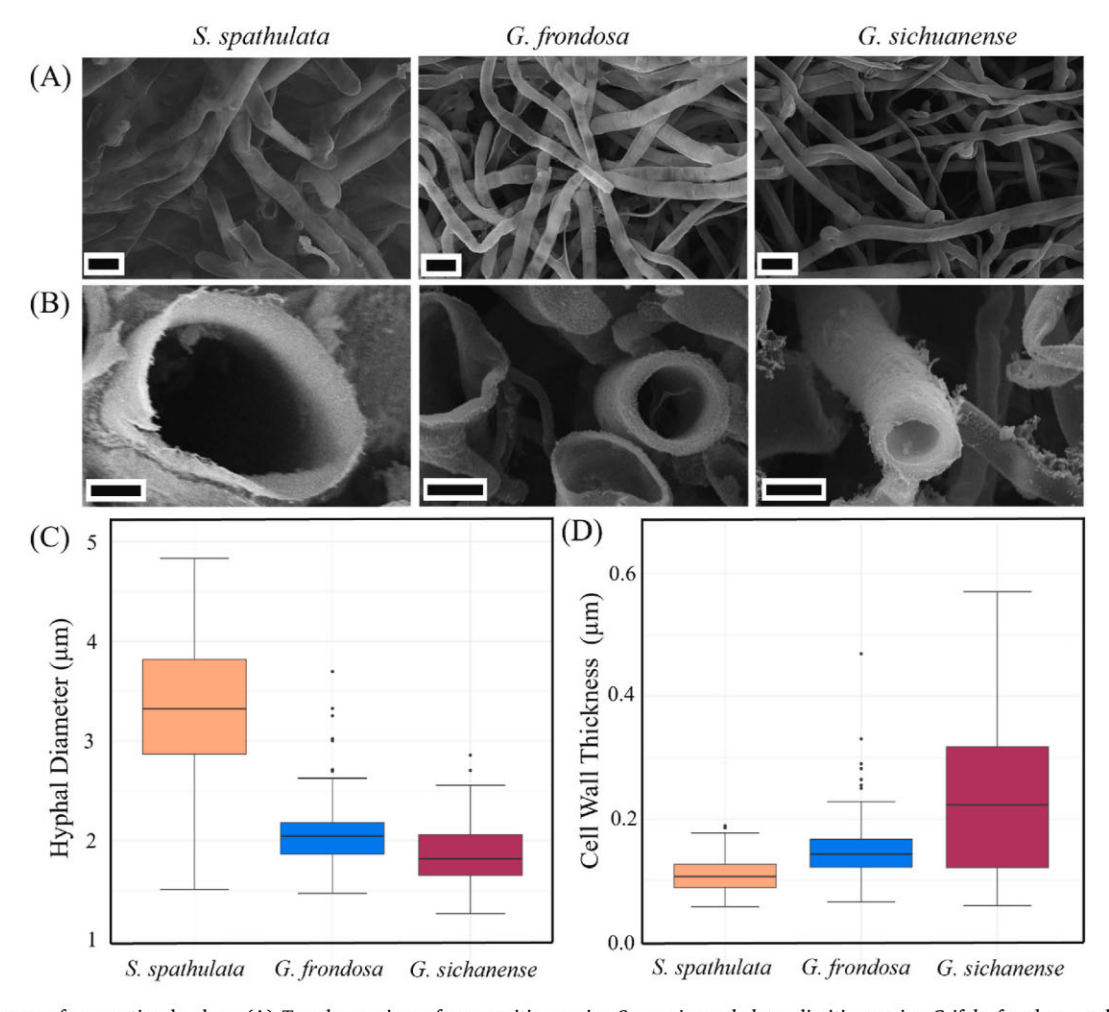


Fig. 2. SEM images of generative hyphae. (A) Top-down view of monomitic species *Sparassis spathulata*, dimitic species *Grifola frondosa*, and trimitic species *Ganoderma sichanense*. Scale bars are 5  $\mu$ m. (B) A cross-sectional view of the cell wall of each species. Scale bars are 1  $\mu$ m. (C) Boxplots comparing the diameters of each species (N = 100). (D) Boxplots comparing the cell wall thickness of each species (N = 100). All pairwise comparisons are statistically significant (p < 0.01) unless noted with same greek letter.

(KP100489.1). The sequence of *Grifola frondosa* culture was identical to five sequences of *Grifola frondosa* in GenBank (MW867037.1, FJ766489.1, MT830900.1, AF324253.1, AY049115.1). The sequence of *Ganoderma sichanense* culture was 99.63 % identical the sequence of the type of *Ganoderma sichuanense* in GenBank (NR\_152892.1). Sequences from the cultures were deposited in GenBank.

# 3.2. Fourier Transform Infrared Spectroscopy

Fig. 1 displays the FTIR data for each of the three species. The data shows that the generative hyphae within the mycelium of all three Polyporales species share the same spectral pattern based on absorption peaks. No peaks were observed that were unique to any one species, indicating no substantial differences in chemical composition. Peaks

Table 2

Microstructural properties of each species generative hyphae including diameter, cell wall thickness, cell wall material volume per hyphal length, and cell wall material volume per hyphae. All data is reported as the mean  $\pm$  one standard deviation. (N = 100). All pairwise comparisions are statistically significant (p < 0.01) unless noted with same greek letter.

| Species                 | Hyphal<br>Diameter<br>(μm) | Cell Wall<br>Thickness<br>(µm)                   | Cell Wall<br>Material<br>Volume Per<br>Hyphal Length<br>(µm <sup>2)</sup> | Cell Wall<br>Material<br>Volume Per<br>Hyphae (%) |
|-------------------------|----------------------------|--|---|---|
| Sparassis<br>spathulata | $3.32 \pm 0.74$            | 0.110 ±<br>0.029                                 | $1.12 \pm 0.44^{\alpha\beta}$   | $13.2\pm3.71$                                     |
| Grifola<br>frondosa     | $2.11\pm0.37$              | $0.153 \pm 0.56$                                 | $0.941\pm0.40^{\beta}$  | $27.2 \pm 9.20$                                   |
| Ganoderma<br>sichanense | $1.87 \pm 0.32$            | $\begin{array}{c} 0.232 \pm \\ 0.13 \end{array}$ | $1.18 \pm 0.70^{\alpha}$  | $42.0\pm18.8$                                     |

associated with lipids, proteins, chitin, and polysaccharides appear to be similar between all three species, suggesting that these species' generative hyphae have the same chemical composition across all three hyphal systems. Of note, this suggests that any observed differences in the structure and properties of the generative hyphae are the result of the microstructural changes, such as amounts of materials associated with cell structure, rather than the chemistry of the material. The spectra displayed in Fig. 1 resemble previous studies describing the chemical composition of other fungi [55,57]. Previous literature using Nuclear Magnetic Resonance (NMR) spectroscopy denoted differences in  $\beta$ -glucan arrangements, specifically the frequency of  $\beta$ -(1,6) glucan side branches along  $\beta$ -(1,3) glucan backbones found in the cell walls, with Grifola frondosa potentially having the highest [58-60]. Higher amounts of these side chains are believed to increase cross-linking between  $\beta$ -(1, 3) glucan backbones and further increase rigidity in cell wall structure [61]. Other studies have shown that there are differences in the amounts of chitin and  $\beta$ -glucan, which can increase rigidity at higher amounts. Ganoderma lucidium, a close relative often used interchangeably with Ganoderma sichuanense, is believed to often have a higher chitin content in its cell walls than Grifola frondosa and potentially Sparassis spathulata [62,63]. These studies emphasize that the quantity of cell wall material rather than material chemistry is often found to be the difference between species.

## 3.3. SEM, hyphal diameter, thickness, and material usage

Fig. 2 shows the images and analysis of the generative hyphal microstructure found between the species of the three hyphal systems. Fig. 2A shows SEM images of generative hyphae from the three species that showed characteristic morphology, such as visible branching and clamp connections. The mycelium of each species appeared as a threadlike network of hyphae with no clear orientation. The observed hyphal networks in the SEM images were consistent with previous studies that examined hyphae from a top-down view [64]. Fig. 2B shows cross-sectional SEM images of the species' cell walls. Of note, there is a clear, subjective decrease in the diameter and increase in the cell wall thickness, moving from monomitic to dimitic to trimitic. Previous works examining the cross-sections of hyphae were not entirely comparable, as they either used light microscopy with staining or, in cases where SEM was used, the hyphae were not fixed and were instead air or freeze-dried [65,66]. Although it is not uncommon for studies to dry fungal cells without applying a fixative, this can lead to changes in shape as water leaves the cells, particularly when the cell membranes or walls have not been fixed in place [47,67]. Though many studies have individually measured the diameters and thicknesses of certain hyphae, there does not appear to be comparative studies of these dimensions based on hyphal system[68-70].

Statistically significant differences were observed in generative

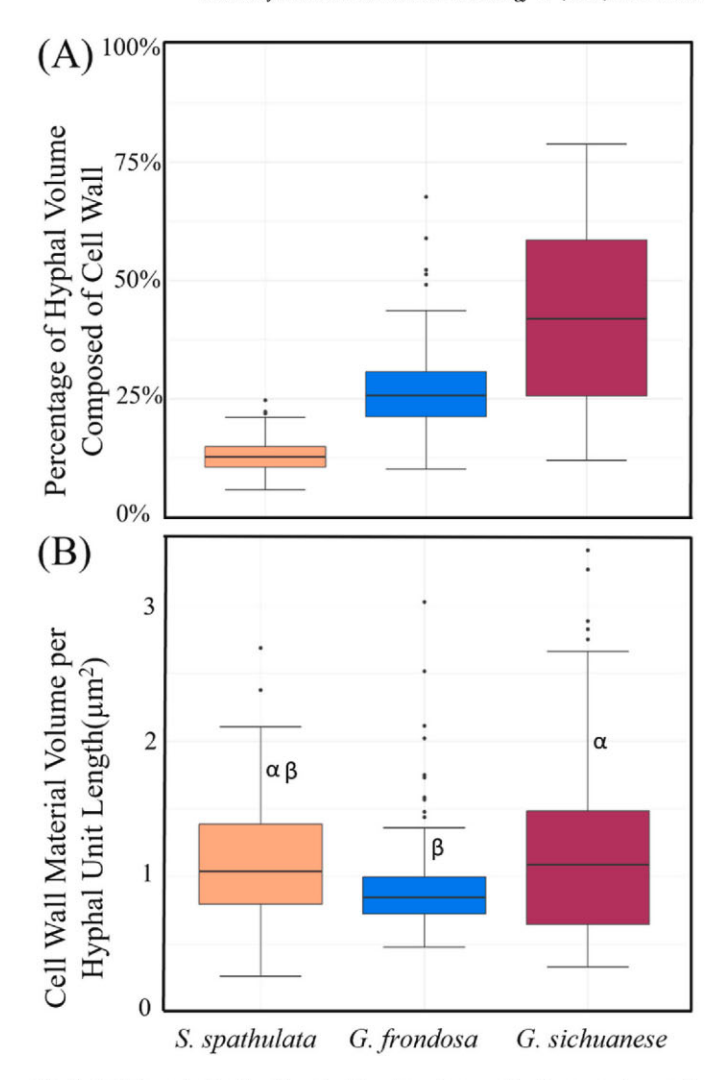


Fig. 3. (A) Percent of cell wall material volume to overall volume used per unit length for each species (N = 100). (D) Cell wall material used per hyphal length (N = 100). All pairwise comparisions are statistically significant (p < 0.01) unless noted with same greek letter.

hyphal diameters (p < 0.01) as shown in Fig. 2C and in cell wall thicknesses (p < 0.01) as shown in Fig. 2D across the three species. Table 2 shows that as the hyphal systems progressed from monomitic to dimitic to trimitic, there was a decrease in generative hyphal diameter while hyphal cell wall thickness increased. Previous literature observing hyphal diameter in Sparassis spathulata measured a range of 4.7-5.8 μm [68], Grifola frondosa to have a range of 2–5 µm [69,71], and Ganoderma sichanense to be around 1.7–3.2 μm [70,72]. These observations support the concept of generative hyphal diameters decreasing as the hyphal systems transition from monomitic to trimitic. The cell wall thickness of Sparassis spathulata and Grifola frondosa do not appear to have been studied at length in previous literature. In contrast, one study found Ganoderma sichanense to have a cell wall thickness of 0.169  $\pm$  0.02  $\mu m$ when studying chemical composition in the fungal cell wall [73]. These past work's diameter measurements are comparable to this study's results but highlight a lack of cell wall thickness measurements. Further study of the cell wall thicknesses and diameters of hyphae would be useful. With both measurements, an estimation of the cell volumes and material usage can be used to explain fungal hyphae's structural properties as shown in this study.

Fig. 3 shows a material compositional analysis of the generative hyphae between the three hyphal systems. Fig. 3A shows the percentage of material volume composed of cell wall per hyphae, which was shown

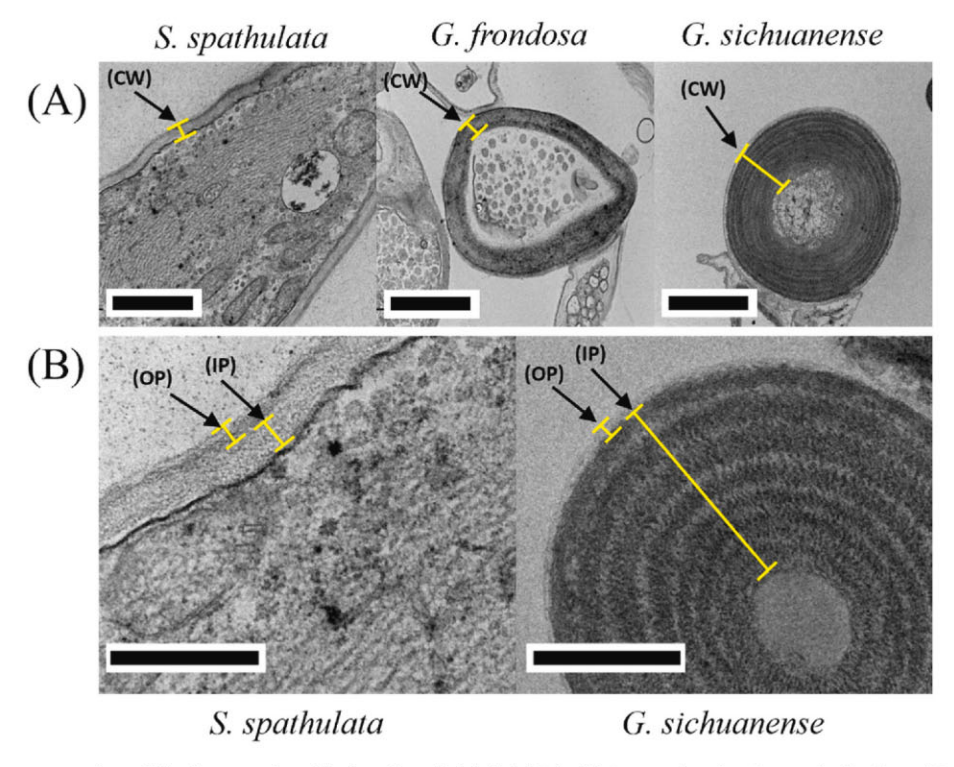


Fig. 4. TEM images of the cross sections of the three species with the cell walls labeled (CW). (A) Images showing Generative hyphae of *Sparassis spathulata* having a thin cell wall and *Grifola frondosa* and especially *Ganoderma sichanense* having thick cell walls. Scale bars are 1 µm. (B) Images showing *Sparassis spathulata* (left) and *Ganoderma sichanense* (right) with a close-up view of their cell wall structure and major portions. The outer portion (OP) of the cell wall is most associated with the mobile phase and is responsible for interacting with the environment. The inner portion (IP) of the cell wall is most associated with the rigid phase and responsible for providing rigidity to the cell. Of note is that *Ganoderma sichuanense's* cell wall emphasized increased thickness in the inner portion responsible for rigidity. Scale bars are 500 nm.

to significantly increase from monomitic to dimitic to trimitic (p < 0.01). As shown in Table 2, Sparassis spathulata appeared to have cell wall material that stayed close to thirteen percent of its total hyphal volume. The variability of Sparassis spathulata was relatively low which shows that there is not a wide range of cell wall thicknesses found in this monomitic species. Alternatively, there were many instances of Grifola frondosa and especially Ganoderma sichanense having cell wall material that made up the majority of the hyphal volume. As shown in Fig. 3B, the actual cell wall material used per hyphae was similar. Both Grifola frondosa and Ganoderma sichanense showed no significant difference (p. > 0.01) in cell wall material to that of Sparassis spathulata. Grifola frondosa and Ganoderma sichanense did show some significant difference (p = 0.0053). Despite showing some significance, this change was small, with a value close to p = 0.01. What was found here is that the generative hyphae of each hyphal system used nearly the same amounts of cell wall material per hyphae. It is then of note that each system's hyphae seem to form a balance between hyphal diameter and cell wall thickness to maintain this consistent cell wall material. Sparassis spathulata seems to grow much larger, thinner generative hyphae while Ganoderma sichanense produces smaller, thicker hyphae while spending the same amount of material per hyphae.

## 3.4. Transmission Electron Microscopy

Fig. 4 displays TEM imaging highlighting the differences in the cell wall structure in between the generative hyphae of the three species. Fig. 4A shows the cell wall structure of the three species and that the thickness increases from monomitic to dimitic to trimitic. Fig. 4B highlights the inner and outer portions of the cell walls in *Sparassis spathulata* and *Ganoderma sichanense*. Sparassis spathulata did not show a large variation in the inner portion of cell wall. In contrast, *Grifola frondosa* and *Ganoderma sichanense* showed increased inner portion cell

wall thickness in their generative hyphae. The inner rigid portion of the cell wall is composed of  $\beta\text{-glucans}$  and chitin and is responsible for rigidity in the cell structure [20,24]. Measurements of the cell walls showed that the inner rigid portions of Ganoderma sichuanense was 351  $\pm$  108 nm and was statistically significantly higher in thickness than that of Grifola frondosa, which had 191  $\pm$  102 nm, and Sparassis spathulata, which had 112  $\pm$  26.3 nm (p < 0.01). Alternatively, Sparassis spathulata had a statistically significantly thicker outer mobile region of 57.3  $\pm$  10.1 nm over that of Ganoderma sichuanense, with 43.1  $\pm$  12.0 nm and Grifola frondosa, with 37.8  $\pm$  20.5 nm (p < 0.01). This means that despite creating smaller hyphae Ganoderma sichanense emphasized the rigid, inner portions of their cell walls in its construction. Of note, this study focused on three Polyporales species due to their close relation, similar chemical compositions and varied toughness. Species of other orders may have different cell wall properties [61].

## 3.5. Mechanical testing

Fig. 5 presents AFM topography and height images of the *Sparassis spathulata*, *Grifola frondosa*, and *Ganoderma sichanense* at regions selected as representative of the mycelia. Fig. 5A indicates multiple strands in each case in height images with height variation across two randomly selected strands depicted in the accompanying graph. Fig. 5B shows the height and stiffness maps of the three tissues. Quantitative images displaying color-coded stiffness maps were generated using a spherical probe with a 100 nm radius, shown in Fig. 5B. These maps reveal the elastic modulus corresponding to surface features at each indentation point, with lighter regions in the QI map indicating higher stiffness values. In each case, a distinct contrast in light pixels is observed between the strands and surrounding areas.

This study examined the mechanical property relationship between species, cell wall characteristics, and stiffness in Polyporales Fungi.

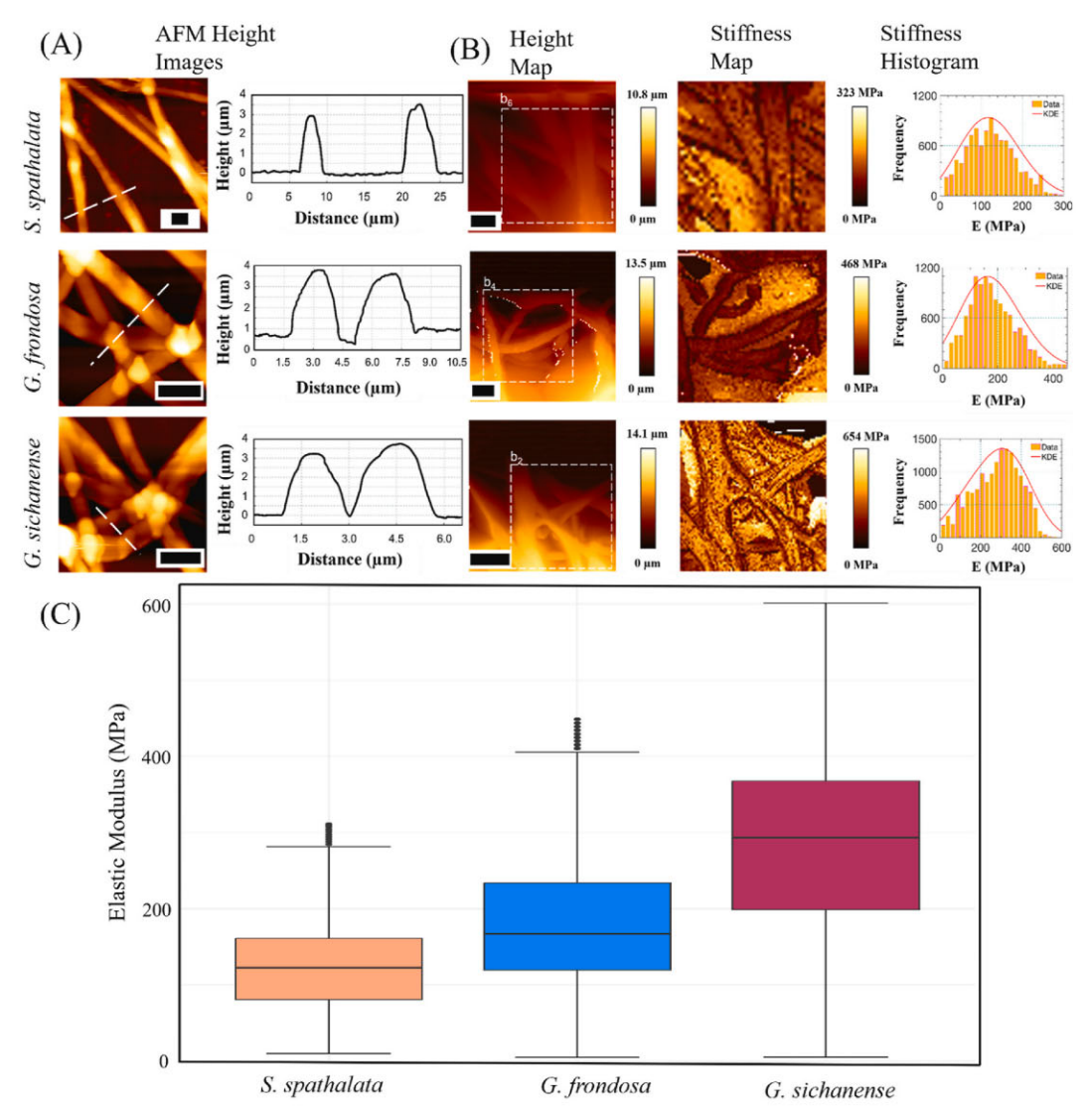


Fig. 5. (A) Ultra-topography tapping mode AFM images of strands from *Sparassis spathulata, Grifola frondosa*, and *Ganoderma sichanense* species. These surface scans were taken from regions of the samples cultured in petri dishes, as identified under light microscopy. The inset highlights the thickness of the fibers. (B) Representative AFM height maps and quantitative stiffness maps are shown with increasing scan resolution, enabling visualization of tissue stiffness and corresponding stiffness histograms. Scale bars for each species are 5  $\mu$ m. (C) Elastic modulus of each species (N > 10000). All pairwise comparisions are statistically significant (p < 0.01) unless noted with same greek letter.

There is not an existing comparison cell wall characteristics as previous work using AFM to analyze fungi focused primarily on the chemical properties of the cell walls and surface proteins but did little to examine the mechanical properties of hyphae [4,19,74]. Fig. 5C shows the elastic moduli of the three species generative hyphae. These findings highlight a substantial difference in the stiffness of each hyphal system compared to one another. As shown in Table 3, Ganoderma sichanense was observed to have an elastic modulus that was significantly higher than that of *Grifola frondosa* (p < 0.01) and *Grifola frondosa* had an elastic modulus that was significantly higher than *Sparassis spathulata* (p < 0.01).

## 3.6. Mechanics and morphology

With fruiting bodies being composed of millions of hyphae, small differences in individual hyphal characteristics may compound, at scale, to affect macroscopic structural characteristics. Results from this study indicate that thicker cell walls cause hyphae to have increased stiffness, providing a basis for a tough structure. Between the hyphal systems, the generative hyphae used similar material types in their microstructures and similar cell wall material usage per hyphae. As shown in Fig. 6, the

allocation of cell wall material was balanced differently to create unique mechanical properties for each species' hyphae. For example, *Ganoderma sichanense's* hyphae were half the diameter, twice the thickness and thus were twice as stiff as the much larger, thinner hyphae of *Sparassis spathulata*. These results highlight that even amongst genetically similar species, generative hyphae can have substantially different microstructures, which must be considered when looking at the mechanical properties of fungi. Identification of hyphal dimensions and cell wall thickening as significant factors in hyphal mechanical properties provides a foundation for further understanding of fungal characteristics, aids in proper species selection in further experiments, and informs future bioinspired design.

## 4. Conclusions

This study compares the generative hyphae of three Polyporales species of fungi that each represent a unique hyphal system to show how differences in their microstructures affect their mechanical properties. This analysis yielded the following results:

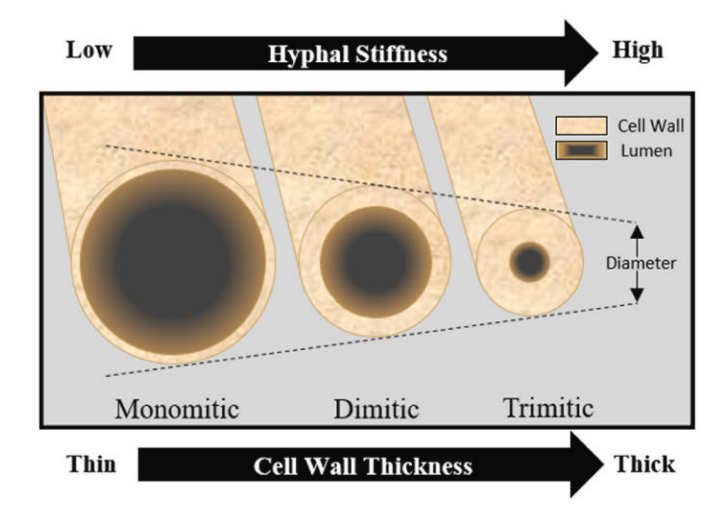


**Fig. 6.** Diagram showing the relationship between hyphal stiffness and dimensions found in three species with different hyphal systems. The cell wall is the structure that encases the fungal cell. The lumen is the enclosed space in the cell containing the organelles and cytoplasm.

**Table 3** Mechanical properties of each species generative hyphae with peak stiffness and elastic modulus. *Note:* Elastic Modulus is reported as the mean  $\pm$  one standard deviation for more than 10,000 measurements. Comparisons that have statistically significant differences (p < 0.01) are labeled with a different Greek letter.

| Species              | Peak Stiffness (MPa) | Elastic Modulus (MPa) |
|----------------------|----------------------|-----------------------|
| Sparassis spathulata | 323                  | $124 \pm 57.3$        |
| Grifola frondosa     | 468                  | $177 \pm 83.4$        |
| Ganoderma sichanense | 654                  | $280\pm115$           |

- (1) FTIR analysis found no substantial chemical differences in the generative hyphae between species, suggesting that the three species are using similar material types in their construction.
- (2) SEM measurements revealed a statistically significant decrease in generative hyphal diameter (p < 0.01), and cell wall thickness statistically significantly increased (p < 0.01) from monomitic to dimitic to trimitic species. Despite this, cell wall material usage per hypha remained consistent while the proportion of hyphal volume occupied by cell wall increased by a statistically significant amount (p < 0.01).
- (3) TEM imaging indicated that the inner rigid portion of the cell wall, responsible for rigidity, increased in thickness from monomitic to trimitic species.
- (4) AFM analysis showed a statistically significant increase (p < 0.01) in generative hyphal stiffness from monomitic to trimitic species.</p>
- (5) Overall, increased cell wall thickness in generative hyphae correlates with greater hyphal stiffness.

## CRediT authorship contribution statement

James A.L. Gallagher: Writing – original draft, Writing – review & editing, Conceptualization, Data curation, Formal analysis, Investigation, Methodology, Visualization. Jessica N. Redmond: Data curation, Writing – review & editing. Meisam Asgari: Investigation, Data curation, Writing – review & editing. Alexander J. Bradshaw: Writing – review & editing. Bryn T.M. Dentinger: Funding acquisition, Resources, Writing – review & editing. Steven E. Naleway: Supervision, Funding acquisition, Conceptualization, Writing – review & editing.

#### Disclaimer

Any opinions, findings, and conclusions or recommendations expressed in this material are those of the author(s) and do not necessarily reflect the views of the National Science Foundation.

#### Data and code availability

Data will be made available on request.

## Supplementary information

Not applicable.

## Ethical approval

Not applicable.

## Declaration of competing interest

The authors declare that they have no known competing financial interests or personal relationships that could have appeared to influence the work reported in this paper.

## Acknowledgments

This material is based upon work supported in part by the National Science Foundation under Grant No. 2233973. The authors of this study would like to thank Nancy Chandler at the University of Utah Electron Microscopy Core Laboratory for all her help during this paper. Thanks goes to Leon Rogers, Sariah VanderVeur, and Toma Ipsen for their mycological expertise. Thanks goes to Hunter Fernandes for his assistance in editing. Big thanks goes to the lead author's partner, Roxanne Johnson, for all her support and artistry.

## References

- Sydor M, Cofta G, Doczekalska B, Bonenberg A. Fungi in mycelium-based composites: usage and recommendations. Materials 2022;15. https://doi.org/ 10.3390/ma15186283.
- [2] Sharma R, Sumbria R. Mycelium bricks and composites for sustainable construction industry: a state-of-the-art review. Innovative Infrastructure Solutions 2022;7:298. https://doi.org/10.1007/s41062-022-00903-y.
- [3] Chakraborty A, Fernando LD, Fang W, Dickwella Widanage MC, Wei P, Jin C, Fontaine T, Latgé JP, Wang T. A molecular vision of fungal cell wall organization by functional genomics and solid-state NMR. Nat Commun 2021;12. https://doi. org/10.1038/s41467-021-26749-z.
- [4] Lateé JP, Wang T. Modern biophysics redefines our understanding of fungal cell wall structure, complexity, and dynamics. mBio 2022;13. https://doi.org/ 10.1128/mbio.01145-22.
- [5] Porter DL, Naleway SE. Hyphal systems and their effect on the mechanical properties of fungal sporocarps. Acta Biomater 2022;145:272–82. https://doi.org/ 10.1016/j.actbio.2022.04.011.
- [6] McGarry A, Burton KS. Mechanical properties of the mushroom, Agaricus bisporus. Mycol Res 1994;98:241–5. https://doi.org/10.1016/S0953-7562(09)80192-5.
- [7] Robertson NF. Presidential address: the fungal hypha. Trans Br Mycol Soc 1965;48:
  1–IN2. https://doi.org/10.1016/S0007-1536(65)80001-8.
- [8] Clark MA, Douglas M, Choi J. Biology 2e. In: OpenStax. second ed. 2018.
- [9] Busch S, Braus GH. How to build a fungal fruit body: from uniform cells to specialized tissue. Mol Microbiol 2007;64:873–6. https://doi.org/10.1111/j.1365-2958.2007.05711.x.
- [10] Haneef M, Ceseracciu L, Canale C, Bayer IS, Heredia-Guerrero JA, Athanassiou A. Advanced materials from fungal mycelium: fabrication and tuning of physical properties. Sci Rep 2017;7. https://doi.org/10.1038/srep41292.
- [11] Appels FVW, Camere S, Montalti M, Karana E, Jansen KMB, Dijksterhuis J, Krijgsheld P, Wösten HAB. Fabrication factors influencing mechanical, moisture-and water-related properties of mycelium-based composites. Mater Des 2019;161: 64–71. https://doi.org/10.1016/j.matdes.2018.11.027.
- [12] Roberson RW, Abril M, Blackwell M, Letcher P, McLaughlin DJ, Mouriño-Pérez RR, Riquelme M, Uchida M. Hyphal structure. In: Cellular and molecular biology of filamentous fungi; 2010. p. 8–24. https://doi.org/10.1128/9781555816636.ch2.
- [13] Gow NAR, Latge J-P, Munro CA. The fungal cell wall: structure, biosynthesis, and function. Microbiol Spectr 2017;5. https://doi.org/10.1128/microbiolspec.funk-0035-2016.

- [14] Beauvais A, Latgé JP. Special issue: fungal cell wall. J Fungi 2018;4. https://doi. org/10.3390/jof4030091.
- [15] Gow NAR, Lenardon MD. Architecture of the dynamic fungal cell wall. Nat Rev Microbiol 2023;21:248–59. https://doi.org/10.1038/s41579-022-00796-9.
- [16] Zabel RA, Morrell JJ. The characteristics and classification of fungi and bacteria. In: Wood microbiology. Elsevier; 2020. p. 55–98. https://doi.org/10.1016/b978-0-12-819465-2.00003-6.
- [17] Grossart H-P, Van den Wyngaert S, Kagami M, Wurzbacher C, Cunliffe M, Rojas-Jimenez K. Fungi in aquatic ecosystems. Nat Rev Microbiol 2019;17:339–54. https://doi.org/10.1038/s41579-019-0175-8.
- [18] Nikitin DA. Ecological characteristics of antarctic fungi, doklady biological sciences, 508; 2023. p. 32–54. https://doi.org/10.1134/S0012496622700120.
- [19] Dufrêne YF. Atomic force microscopy of fungal cell walls: an update. Yeast 2010; 27:465–71. https://doi.org/10.1002/yea.1773.
- [20] Ene IV, Walker LA, Schiavone M, Lee KK, Martin-Yken H, Dague E, Gow NAR, Munro CA, Brown AJP. Cell wall remodeling enzymes modulate fungal cell wall elasticity and osmotic stress resistance. mBio 2015;6. https://doi.org/10.1128/ mBio 00086.15
- [21] Watkinson SC, Boddy L, Money NP. The fungi. third ed. 2015.
- [22] Mykchaylova O, Lomberg M. Microstructures of vegetative mycelium of macromycetes in pure cultures. 2009. https://www.researchgate.net/publication/ 292406879.
- [23] Money NP. Mushroom stem cells. Bioessays 2002;24:949–52. https://doi.org/ 10.1002/bies.10160.
- [24] Fernando LD, Pérez-Llano Y, Dickwella Widanage MC, Jacob A, Martínez-Ávila L, Lipton AS, Gunde-Cimerman N, Latgé JP, Batista-García RA, Wang T. Structural adaptation of fungal cell wall in hypersaline environment. Nat Commun 2023;14. https://doi.org/10.1038/s41467-023-42693-6.
- [25] Leif Ryvarden. The polyporaceae of North Europe. Oslo, Norway: Fungiflora; 1976.
- [26] Sumbali G. The fungi. Alpha Science International Ltd; 2005.
- [27] Blackwell MM, Alexopoulos, Constantine J, Mims CW. Introductory mycology. fourth ed., fourth ed. 1996.
- [28] Clémençon H. Cytology and plectology of the hymenomycetes. Bibliotheca Mycologica; 2004.
- [29] Corner EJH. A Fomes with two systems of hyphae. Trans Br Mycol Soc 1932;17: 51–81. https://doi.org/10.1016/S0007-1536(32)80026-4.
- [30] Corner EJH. The construction of Polypores. 1953. https://lib.utah.edu/services/course-reserves.phporcontact801.
- [31] Porter DL, Hotz E, Uehling J, Naleway S. A review of the material and mechanical properties of select Ganoderma fungi structures as a source for bioinspiration. J Mater Sci 2023;58:1–20. https://doi.org/10.1007/s10853-023-08214-y.
- [32] Chan XY, Saeidi N, Javadian A, Hebel DE, Gupta M. Mechanical properties of dense mycelium-bound composites under accelerated tropical weathering conditions. Sci Rep. 2021;11. https://doi.org/10.1038/s41598-021-01598-4.
- [33] Zhou JL, Zhu L, Chen H, Cui BK. Taxonomy and phylogeny of polyporus group melanopus (Polyporales, basidiomycota) from China. PLoS One 2016;11. https:// doi.org/10.1371/journal.pone.0159495.
- [34] Læssøe T, Petersen JH. Fungi of temperate Europe. Princeton University Press; 2019.
- [35] Mycelium Emporium, (n.d.). https://www.themyceliumemporium.com/(accessed September 24, 2024).
- [36] Grand LF. Grifola frondosa (Dicks.) gray. 2011.
- Schoch CL, Seifert KA, Huhndorf S, Robert V, Spouge JL, Levesque CA, Chen W, Bolchacova E, Voigt K, Crous PW, Miller AN, Wingfield MJ, Aime MC, An KD, Bai FY, Barreto RW, Begerow D, Bergeron MJ, Blackwell M, Boekhout T, Bogale M, Boonyuen N, Burgaz AR, Buyck B, Cai L, Cai Q, Cardinali G, Chaverri P, Coppins BJ, Crespo A, Cubas P, Cummings C, Damm U, de Beer ZW, de Hoog GS, Del-Prado R, Dentinger B, Diéguez-Uribeondo J, Divakar PK, Douglas B, Dueñas M, Duong TA, Eberhardt U, Edwards JE, Elshahed MS, Fliegerova K, Furtado M, García MA, Ge ZW, Griffith GW, Griffiths K, Groenewald JZ, Groenewald M, Grube M, Gryzenhout M, Guo LD, Hagen F, Hambleton S, Hamelin RC, Hansen K, Harrold P, Heller G, Herrera C, Hirayama K, Hirooka Y, Ho HM, Hoffmann K, Hofstetter V, Högnabba F, Hollingsworth PM, Hong SB, Hosaka K, Houbraken J, Hughes K, Huhtinen S, Hyde KD, James T, Johnson EM, Johnson JE, Johnston PR, Jones EBG, Kelly LJ, Kirk PM, Knapp DG, Kõljalg U, Kovács GM, Kurtzman CP, Landvik S, Leavitt SD, Liggenstoffer AS, Liimatainen K, Lombard L, Luangsa-ard JJ, Lumbsch HT, Maganti H, Maharachchikumbura SSN, Martin MP, May TW, McTaggart AR, Methven AS, Meyer W, Moncalvo JM, Mongkolsamrit S, Nagy LG, Nilsson RH, Niskanen T, Nyilasi I, Okada G, Okane I, Olariaga I, Otte J, Papp T, Park D, Petkovits T, Pino-Bodas R, Quaedvlieg W, Raja HA, Redecker D, Rintoul TL, Ruibal C, Sarmiento-Ramírez JM, Schmitt I, Schüßler A, Shearer C, Sotome K, Stefani FOP, Stenroos S, Stielow B, Stockinger H, Suetrong S, Suh SO, Sung GH, Suzuki M, Tanaka K, Tedersoo L, Telleria MT, Tretter E, Untereiner WA, Urbina H, Vágvölgyi C, Vialle A, Vu TD, Walther G, Wang QM, Wang Y, Weir BS, Weiß M, White MM, Xu J, Yahr R, Yang ZL, Yurkov A, Zamora JC, Zhang N, Zhuang WY, Schindel D. Nuclear ribosomal internal transcribed spacer (ITS) region as a universal DNA barcode marker for Fungi. Proc Natl Acad Sci U S A 2012;109: 6241-6. https://doi.org/10.1073/pnas.1117018109.
- [38] Bradshaw AJ, Backman TA, Ramírez-Cruz V, Forrister DL, Winter JM, Guzmán-Dávalos L, Furci G, Stamets P, Dentinger BTM. DNA authentication and chemical analysis of psilocybe mushrooms reveal widespread misdeterminations in fungaria and inconsistencies in metabolites. Appl Environ Microbiol 2022;88. https://doi.org/10.1128/aem.01498-22.
- [39] Dentinger BTM, Margaritescu S, Moncalvo JM. Rapid and reliable high-throughput methods of DNA extraction for use in barcoding and molecular systematics of

- mushrooms. Mol Ecol Resour 2010;10:628–33. https://doi.org/10.1111/j.1755-0998.2009.02825.x.
- [40] Camacho C, Coulouris G, Avagyan V, Ma N, Papadopoulos J, Bealer K, Madden TL. BLAST+: architecture and applications. BMC Bioinf 2009;10. https://doi.org/ 10.1186/1471-2105-10-421.
- [41] Sayers EW, Cavanaugh M, Clark K, Ostell J, Pruitt KD, Karsch-Mizrachi I. GenBank. Nucleic Acids Res 2020;48:D84–6. https://doi.org/10.1093/nar/gkz956.
- [42] Aryal S. Potato dextrose agar (PDA)- principle, uses, composition, procedure and colony characteristics. Microbiology Info Com 2022. https://microbiologyinfo. com/potato-dextrose-agar-pda-principle-uses-composition-procedure-and-colo ny-characteristics/. [Accessed 14 July 2024].
- [43] De Wet MMM, Brink HG. Fungi in the bioremediation of toxic effluents. In: Fungi bio-prospects in sustainable agriculture, environment and nano-technology: volume 2: extremophilic fungi and myco-mediated environmental management. Elsevier; 2020. p. 407–31. https://doi.org/10.1016/B978-0-12-821925-6.00018-6.
- [44] Gwon JH, Park H, Eom AH. Effect of temperature, pH, and media on the mycelial growth of tuber koreanum. MYCOBIOLOGY 2022;50:238–43. https://doi.org/ 10.1080/12298093.2022.2112586.
- [45] De Ligne L, Vidal-Diez de Ulzurrun G, Baetens JM, Van den Bulcke J, Van Acker J, De Baets B. Analysis of spatio-temporal fungal growth dynamics under different environmental conditions. IMA Fungus 2019;10. https://doi.org/10.1186/s43008-019-0009-3.
- [46] Aleklett K, Boddy L. Fungal behaviour: a new frontier in behavioural ecology. Trends Ecol Evol 2021;36:787–96. https://doi.org/10.1016/j.tree.2021.05.006.
- [47] Murtey MD, Ramasamy P. Life science sample preparations for scanning electron microscopy. 2021.
- [48] Graham L, Orenstein JM. Processing tissue and cells for transmission electron microscopy in diagnostic pathology and research. Nat Protoc 2007;2:2439–50. https://doi.org/10.1038/nprot.2007.304.
- [49] Gorbushina AA, Whitehead K, Dornieden T, Niesse A, Schulte A, Hedges JI. Black fungal colonies as units of survival: hyphal mycosporines synthesized by rockdwelling microcolonial fungi. Can J Bot 2003;81:131–8. https://doi.org/10.1139/ b03-011.
- [50] Asgari M, Brulé V, Western TL, Pasini D. Nano-indentation reveals a potential role for gradients of cell wall stiffness in directional movement of the resurrection plant Selaginella lepidophylla. Sci Rep 2020;10. https://doi.org/10.1038/s41598-019-57365-2
- [51] Brulé V, Rafsanjani A, Asgari M, Western TL, Pasini D. Three-dimensional functional gradients direct stem curling in the resurrection plant Selaginella lepidophylla. J R Soc Interface 2019:16. https://doi.org/10.1098/rsif.2019.0454.
- [52] Asgari M, Latifi N, Giovanniello F, Espinosa HD, Amabili M. Revealing layer-specific ultrastructure and nanomechanics of fibrillar collagen in human aorta via atomic force microscopy testing: implications on tissue mechanics at macroscopic scale. Adv Nanobiomed Res 2022;2. https://doi.org/10.1002/anbr.202100159.
- [53] Hutter JL, Bechhoefer J. Calibration of atomic-force microscope tips. Rev Sci Instrum 1993;64:1868–73. https://doi.org/10.1063/1.1143970.
- [54] H.H. Von Herrn, Ueber die Berührung fester elastischer Körper, (n.d.).
- [55] Huleihel M, Shufan E, Tsror L, Sharaha U, Lapidot I, Mordechai S, Salman A. Differentiation of mixed soil-borne fungi in the genus level using infrared spectroscopy and multivariate analysis. J Photochem Photobiol, B 2018;180: 155–65. https://doi.org/10.1016/j.jphotobiol.2018.02.007.
- [56] Salman A, Tsror L, Pomerantz A, Moreh R, Mordechai S, Huleihel M. FTIR spectroscopy for detection and identification of fungal phytopathogenes. Spectroscopy 2010;24:261–7. https://doi.org/10.3233/SPE-2010-0448.
- [57] Fransson P, Robertson AHJ, Campbell CD. Carbon availability affects already large species-specific differences in chemical composition of ectomycorrhizal fungal mycelia in pure culture. Mycorrhiza 2023;33:303–19. https://doi.org/10.1007/ s00572-023-01128-2.
- [58] Fang J, Wang Y, Lv X, Shen X, Ni X, Ding K. Structure of a β-glucan from Grifola frondosa and its antitumor effect by activating Dectin-1/Syk/NF-κB signaling. Glycoconj J 2012;29:365–77. https://doi.org/10.1007/s10719-012-9416-z.
- [59] Wang J, Yuan Y, Yue T. Immunostimulatory activities of β-d-glucan from ganoderma lucidum. Carbohydr Polym 2014;102:47–54. https://doi.org/10.1016/ j.carbpol.2013.10.087.
- [60] Yang YH, Kang HW, Ro HS. Cloning and molecular characterization of β-1,3-glucan synthase from sparassis crispa. MYCOBIOLOGY 2014;42:167–73. https://doi.org/ 10.5941/MYCO.2014.42.2.167.
- [61] Free SJ. Fungal cell wall organization and biosynthesis. In: Adv genet. Academic Press Inc.; 2013. p. 33–82. https://doi.org/10.1016/B978-0-12-407677-8.00002-6
- [62] Ospina Álvarez SP, Ramírez Cadavid DA, Escobar Sierra DM, Ossa Orozco CP, Rojas Vahos DF, Zapata Ocampo P, Atehortúa L. Comparison of extraction methods of chitin from ganoderma lucidum mushroom obtained in submerged culture. BioMed Res Int 2014;2014. https://doi.org/10.1155/2014/169071.
- [63] Nitschke J, Altenbach HJ, Malolepszy T, Mölleken H. A new method for the quantification of chitin and chitosan in edible mushrooms. Carbohydr Res 2011; 346:1307–10. https://doi.org/10.1016/j.carres.2011.03.040.
- [64] Islam MR, Tudryn G, Bucinell R, Schadler L, Picu RC. Morphology and mechanics of fungal mycelium. Sci Rep 2017;7. https://doi.org/10.1038/s41598-017-13295-2.
- [65] Howard RJ. Ultrastructural analysis of hyphal tip cell growth in fungi: SPITZENKORPER, cytoskeleton and endomembranes after freeze-substitution. 1981.
- [66] Chen H, Abdullayev A, Bekheet MF, Schmidt B, Regler I, Pohl C, Vakifahmetoglu C, Czasny M, Kamm PH, Meyer V, Gurlo A, Simon U. Extrusion-based additive manufacturing of fungal-based composite materials using the tinder fungus Fomes

- fomentarius. Fungal Biol Biotechnol 2021;8. https://doi.org/10.1186/s40694-021-00120.0
- [67] Brunk U, Collins VP, Arro E. The fixation, dehydration, drying and coating of cultured cells for SEM. J Microsc 1981;123:121–31. https://doi.org/10.1111/ j.1365-2818.1981.tb01288.x.
- [68] Light W, Woehrel M. Clarification of the nomenclatural confusion of the genus Sparassis [Polyporales: sparassidaceae]. North America; 2009. http://www.indexfungorum.org/Names/Names.asp.
- [69] Tang SM, Chen DC, Wang S, Wu XQ, Ao CC, Li EX, Luo HM, Li SH. Morphological and molecular analyses reveal two new species of Grifola (Polyporales) from Yunnan, China. MycoKeys 2024;102:267–84. https://doi.org/10.3897/ mycokeys.102.118518.
- [70] Luangharn T, Karunarathna SC, Dutta AK, Paloi S, Promputtha I, Hyde KD, Xu J, Mortimer PE. Ganoderma (Ganodermataceae, basidiomycota) species from the greater mekong subregion. J Fungi 2021;7. https://doi.org/10.3390/jof7100819.
- [71] Shen Q. MOLECULAR phylogenetic analysis of grifola frondosa (maitake) and related species and the influence of selected nutrient supplements on mushroom yield A thesis. Plant Pathol 2001.
- [72] Bhosle S, Ranadive K, Bapat G, Garad S, Deshpande G, Vaidya J. Taxonomy and diversity of Ganoderma from the Western parts of Maharashtra (India). 2010. www .punjabenvironment.com/bd\_list.htm.
- [73] Ma Z, Xu M, Wang Q, Wang F, Zheng H, Gu Z, Li Y, Shi G, Ding Z. Development of an efficient strategy to improve extracellular polysaccharide production of ganoderma lucidum using L-phenylalanine as an enhancer. Front Microbiol 2019; 10. https://doi.org/10.3389/fmicb.2019.02306.
- [74] McMaster TJ. Atomic Force Microscopy of the fungi-mineral interface: applications in mineral dissolution, weathering and biogeochemistry. Curr Opin Biotechnol 2012;23:562–9. https://doi.org/10.1016/j.copbio.2012.05.006.